

# Rethinking Programmed I/O for Fast Devices, Cheap Cores, and Coherent Interconnects

Anastasiia Ruzhanskaia  
Systems Group, D-INFK, ETH Zürich  
Zürich, Switzerland

David Cock  
Systems Group, D-INFK, ETH Zürich  
Zürich, Switzerland

Pengcheng Xu  
Systems Group, D-INFK, ETH Zürich  
Zürich, Switzerland

Timothy Roscoe  
Systems Group, D-INFK, ETH Zürich  
Zürich, Switzerland

## Abstract

Conventional wisdom holds that an efficient interface between an OS running on a CPU and a high-bandwidth I/O device should be based on Direct Memory Access (DMA), descriptor rings, and interrupts: DMA offloads transfers from the CPU, descriptor rings provide buffering and queuing, and interrupts facilitate asynchronous interaction between cores and device with a lightweight notification mechanism.

In this paper we question this wisdom in the light of modern hardware and workloads, particularly in cloud servers. We argue that the assumptions that led to this model are obsolete, and in many use-cases use of *programmed I/O*, where the CPU explicitly transfers data and control information to and from a device via loads and stores, actually results in a more efficient system.

We quantitatively demonstrate these advantages using three use-cases: fine-grained RPC-style invocation of functions on an accelerator, offloading of operators in a streaming dataflow engine, and a network interface targeting for serverless functions. Moreover, we show that while these advantages are significant over a modern PCI Express (PCIe) peripheral bus, a truly cache-coherent interconnect offers significant additional efficiency gains.

## 1 Introduction

There is a current consensus on how CPUs should communicate with modern, high-performance devices like network interface adaptors (NICs), storage controllers, Graphics Processing Units (GPUs), and other computational accelerators: for the most part, this is achieved using DMA and rings of descriptors to decouple CPU and device as much as possible. On modern PCIe interconnects, this consensus results in impressive bandwidth for applications which transfer data in large chunks.

However, in this paper we question this consensus in the light of several factors: (1) important workloads involving irregular access and fine-grained interaction between CPU and device, (2) increasing core counts in servers, (3) data center applications where many machines are executing the same application on most of their cores, and (4) the emergence of cache-coherent peripheral interconnects, particularly those

like CXL.cache 3.0 [15] in which devices are first-class participants in the coherence protocol.

We argue that these factors make *Programmed I/O (PIO)*, where CPU software performs I/O by directly reading and writing device registers, a better mechanism for data transfer in some important scenarios than one based on DMA.

We use a real hardware platform which implements a coherent interconnect between a server-class CPU and a large FPGA to investigate the trade-offs between DMA using descriptor rings, PIO directly over a PCIe interconnect, and PIO over a cache-coherence protocol.

We show that, for small (around 1KiB or less) transfers, PIO posted *writes* over PCIe significantly outperform DMA, although *reads* are less efficient since, unlike writes, they cannot be pipelined and so incur PCIe’s significant round-trip latency penalty. However, a full cache coherence protocol which avoids PCIe significantly outperforms both DMA and PIO over PCIe.

We go further, however, and show how a conventional MESI-like coherence protocol can be *exploited in novel ways* by intelligent devices which can interact with an unmodified CPU at the coherence message level. By *relaxing traditional coherence protocol assumptions* (for example, the independence of cache lines), we can achieve dramatically more efficient communication between a CPU and a device.

In the following section, we provide background and motivation for this work, including the factors that led to the descriptor-based DMA model of I/O, and why it is time to question the underlying assumptions in that model. In [Section 3](#) we describe and motivate the experimental hardware platform we use for our evaluation, and also provide calibrating performance comparisons with PC data center servers.

In [Section 4](#), we discuss why true cache-coherent device interconnects are fundamentally different from today’s PCIe platforms, and present a set of efficient protocols for passing messages with low latency between software running on an unmodified CPU, and a smart device which has low-level access to the coherence protocol. In [Section 4.5](#), we go on to present the implementation of some of these protocols on our experimental platform.

[Section 5](#) then compares a traditional DMA-based approach with PIO over PCIe and our new coherence-based

protocols using three different use-cases: (1) lightweight, synchronous local invocation of functionality on a computational accelerator, (2) I/O to and from an intelligent network interface, and (3) hardware offload of a distributed dataflow stream processor to an FPGA. We survey related work in Section 6 and conclude with Section 7.

## 2 Background and Motivation

Our work in this paper is motivated by the interaction between modern trends in platform interconnect and also the changing ways in which these interconnects are used, particularly in data center and cloud servers.

### 2.1 Background: hardware/software interaction

In early machines, the CPU interacted with peripheral devices exclusively using *programmed I/O* (PIO): the device exposed hardware registers mapped into the processor’s address space. Both data transfer and control of the device involved reads and writes by the CPU to these registers.

This model made sense when devices were extremely simple, particularly when augmented by the use of device interrupts to obviate the need for the CPU to poll status registers on the device waiting for an I/O operation to complete. However, the model still requires a synchronous rendezvous between the CPU and device, and moreover requires all data to be transferred via CPU registers (since the CPU is copying data between device registers and main memory).

DMA removes this limitation by allowing the device itself or a dedicated DMA controller to copy the data while the CPU continues to execute other code, providing parallelism and partly decoupling the CPU and device. Further decoupling is provided by *descriptor rings*: producer/consumer buffers of I/O requests in memory represented as a queue of operations, and read and written by both the CPU and the DMA-capable device. In this case, interrupts need only be used when the queue of descriptors becomes full or empty.

Almost every high-speed device today uses essentially this technique, with minor variations such as how the descriptor queues are formatted, where they are stored, and whether the head and tail of the queue is identified by registers or flags in the descriptors themselves.

This model is optimized for throughput – it is most efficient when a large volume of data must be transferred.

### 2.2 Trends in interconnects and devices

The evolution of peripheral interconnects has paralleled that of device programming towards high-throughput, decoupled designs that minimize interaction with the CPU during I/O operations. Modern PCIe links offer very high transfer throughput. Surprisingly, increasing state-of-the-art PCIe throughput over time has not been accompanied by a corresponding reduction in *latency*, which has remained a roughly

1 $\mu$ s for an interconnect round-trip message exchange. However, for the large batch transfers used in GPU-derived programming models for, e.g., machine learning workloads this latency penalty is insignificant when amortized over a large transfer, and indeed such software has arguably adapted to this model imposed by the hardware [23].

Recent trends in accelerator design, however, have led to proposed standards for *cache coherent* peripheral interconnects, and the related idea of extending processor cache coherence to heterogeneous devices: accelerators, networking interfaces, and storage controllers [4, 11, 16, 39, 45]. The more far-reaching of these proposals are fully *symmetric*, i.e. devices are first-class participants in a distributed directory-based cache coherence protocol.

Communication in software between peer modes in a cache-coherent system is typically very different from using descriptor-based DMA. FastForward [18], Barrelfish’ UMP [5], Concord [26], and Shinjuku [28] adopt a much more direct approach to sending small messages with low latency, e.g. by exploiting the cache coherence protocol to transfer lines between caches on demand, and local polling to provide synchronization. Recently, cache coherence between NUMA CPUs has been used to *simulate* communicating between software and a hypothetical cache-coherent NIC [43].

### 2.3 “New” workloads

Without denying the importance of throughput-oriented data transfer between devices and cores for workloads like current machine learning training and inference, it is worth stepping back and questioning many of the assumptions that led us here, and what other workloads might be a poor fit today for this model.

Any workload involving fine-grained, frequent interaction between the CPU and another device incurs a significant latency penalty when using DMA for data transfer. Many irregular workloads have this property [7, 21, 30, 52].

Moreover, data center messaging (essentially, network Remote Procedure Calls (RPCs)) exchange many small messages [29, 33]. While end-to-end latency is mostly network propagation time in this case, latency incurred in the end system is a good proxy for resources (such as CPU cycles) wasted before invoking the application code, and in marshaling and sending any reply.

There are also several assumptions underlying the DMA-based communication model which are worth revisiting. In particular, CPU execution and I/O were decoupled because CPU cycles were precious (there being few cores), and the CPU had plenty of different tasks to work on at any time.

This is no longer true. Server CPUs have had many cores for some time, and moreover when running data center applications they are often dedicated to a single application, sometimes with miscellaneous functions moved to a small subset of the cores [35].

Another example: for throughput-oriented workloads DMA has evolved to efficiently transfer data to and from main memory without polluting the CPU cache. However, for small message applications, it is important that almost all the data gets into the right CPU cache as quickly as possible.

This leads us to rethink the use of the DMA model, and whether directly involving the CPU in data transfers to and from devices might be a better approach for many scenarios on modern hardware. Others have also suggested this in some cases [12, 32], but we also push the question much further: given a future cache-coherent interconnect, what *new ways of using Programmed I/O* might become compelling for data center applications.

### 3 Experimental platform

We investigate the modern trade-offs between PIO, DMA, and cache-coherent interconnects using the Enzian research computer [13]. Enzian is useful as a placeholder for future, interoperable, cache-coherent interconnects like CXL.

We use a real hardware platform rather than a simulator. Simulation would be appropriate for detailed quantitative comparisons of known techniques, but in this paper we explore unconventional uses of cache coherence and so want to establish not only that our techniques are performant, but that they can practically be implemented in a real system.

An Enzian machine can be thought of as a two-socket NUMA server, where one socket houses a Marvel Cavium ThunderX-1 CPU, with a Xilinx XCVU9P FPGA in the other.

The CPU is a 48-core ARMv8 processor running at 2.0GHz, and 128GiB of 2133MT/s DDR4 memory spread across 4 memory controllers. Each core has a 32KiB, 32-way associative, write-through, physically indexed, physically tagged, L1 data cache. These are connected to a 16MiB, write-back, 16-way associative, shared L2 last-level cache. Hardware keeps the L1 caches coherent with the L2, and so in ARM architecture parlance the point of coherence is the L1 cache, whereas the point of unification is the L2 cache write-through. The cache-line size is 128 bytes – note that this is double the conventional 64-byte line size.

The CPU and FPGA are connected by the CPU’s native inter-socket cache coherent protocol, the Enzian Coherence Interface (ECI), which Enzian implements on the FPGA. It is a MOESI-like directory based protocol, and the physical address space is statically partitioned between the two NUMA nodes (CPU and FPGA). It uses 24 bidirectional lanes (organized into 2 12-lane links), each running at about 10Gb/s, for a theoretical inter-socket bandwidth of about 30GiB/s.

Both nodes have PCIe interfaces: the ThunderX-1 has a PCIe Gen.3 x8 interface, while the FPGA has a PCIe Gen.3 x16 interface. In this work we connect these two interfaces with a loopback cable; this essentially replicates the case of an PCIe accelerator card and allows us to compare PCIe with ECI in our experiments.

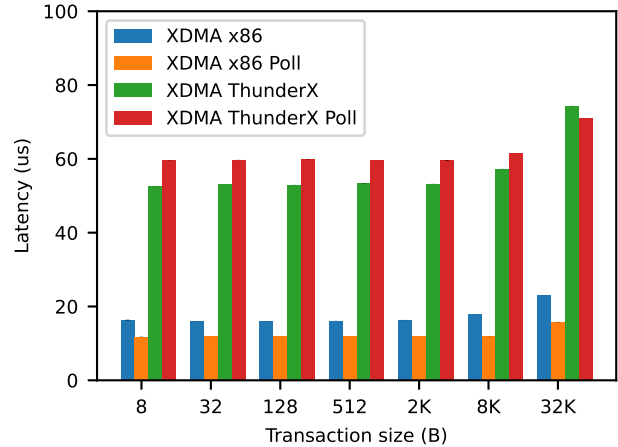


**Figure 1.** Comparison of XDMA latency for RPC workload between Enzian and PC

#### 3.1 Characterizing the platform

Enzian provides a real hardware platform with server-class performance to evaluate different forms of device communication. However, direct comparisons with modern server platforms is not straightforward: the latter do not offer a full cache coherence protocol between the CPU and devices, but do provide more recent and therefore higher-performance cores, memory systems, and PCIe interconnects.

Therefore, in order to calibrate against a modern PC for both PIO and DMA over PCIe, we present two benchmark comparisons of Enzian with a modern PC (Intel Core i7-7700 3.6GHz Kaby Lake, PCIe Gen.3 x16) with cache line size of 64 bits connected to an AMD Xilinx Virtex UltraScale+ VCU118 card, using the same “write then read” experiment detailed in Section 5.1. The VCU118 uses the same FPGA as Enzian, albeit a slightly slower speed gauge.

**3.1.1 DMA performance over PCIe.** The first experiment uses DMA, using the Xilinx XDMA IP and associated descriptor-based protocol to transfer data between the CPU and the FPGA over PCIe. Figure 1 shows results for various data transfer sizes, running the Xilinx driver in both interrupt-driven and polled modes.

We observe that, using PCIe, exchanging messages using XDMA is about 3 times as fast on the PC server than on Enzian, while the difference between interrupt-driven and polling performance is much less significant. The latency of a single transaction is pretty constant on both platforms up to the PCIe transaction size limit of 4KiB, and then increases.

The difference in performance between the two architectures is due to several factors. For very small transfers, the CPU overhead of setting up descriptors dominates, and an x86 core is simply faster than the slower (and mostly in-order) ThunderX-1 core. In addition, the memory system is

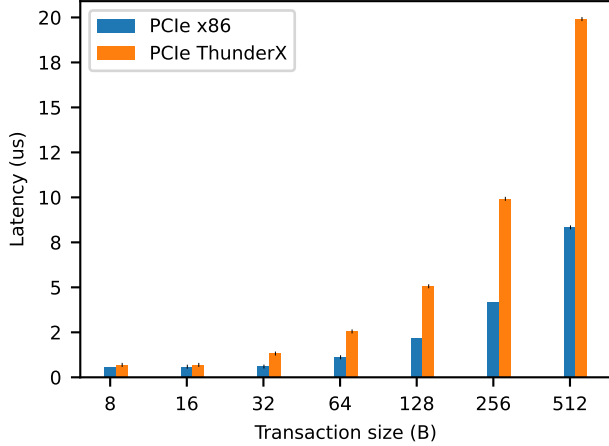


**Figure 2.** Comparison of PIO latency for RPC workload between Enzian and PC

somewhat faster on the PC. The factor of 2 difference in PCIe *bandwidth* between the two platforms does not appear to be a factor in these experiments.

**3.1.2 PIO performance over PCIe.** Our second calibration experiment involves the CPU itself doing PIO reads and writes over PCIe to the FPGA.

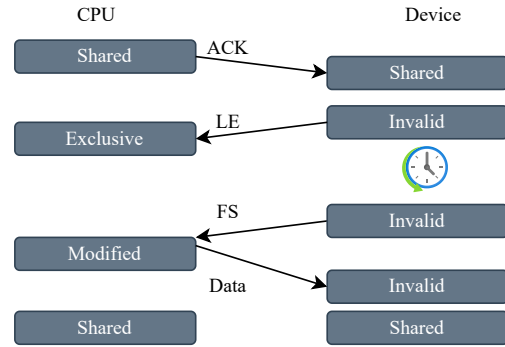
We experimented with several different optimizations in this experiment, in particular the use of write combining and vector instructions. We present the best figures we could obtain on both platforms.

Figure 2 shows the results. For transaction sizes above 32 bytes, the PC is about twice as fast as Enzian over the PCIe cable between CPU and FPGA. Here, the factor of 2 difference in PCIe bandwidth is responsible for the latency difference, in particular for reads (which are limited to 128 bits on both platforms). Writes, in contrast, are combined and highly pipelined at the PCIe interface.

## 4 Programmed I/O over coherent interconnects

In this section we explore what programmed I/O might look over coherent interconnects. It is of course possible for a CPU to simply copy data over a coherent interconnect as in conventional programmed I/O. This requires careful management of the processor’s cache hierarchy with explicit cache flush and invalidate instructions, but can be appropriate when the underlying hardware standard itself mandates a cache on the device, as with OpenCAPI 4.0 [1, 45].

That said, here we are more interested in how a coherent interconnect can best be used for low-latency, efficient movement of data between CPU registers and a device, including cases where the conventional notion of the cache



**Figure 3.** Simple inter-core communication over coherence

as a view over memory contents is not appropriate (such as data arriving over a network).

We scope the question further as follows: we consider the case where the CPU cores, or their Last-Level Cache (LLC), communicate with devices via a MESI-like [37], message-based coherence protocol with stable states corresponding to MODIFIED (dirty), SHARED (clean), EXCLUSIVE (clean), and INVALID, using a distributed cache directory. Note that this means that each address or cache line has a *home node*, which maintains the directory entry for the line.

Moreover, we assume a *symmetric* protocol: each device is a first-class participant in the protocol with a subset of physical addresses homed at it, and the device therefore maintains directory state for these lines.

While these assumptions are rare in hardware today, they are true both of the proposed CXL.cache standard [15] and the Enzian platform we use for experiments.

### 4.1 Baseline: naively communicating with coherence

Our starting point is existing techniques which use cache coherence to perform inter-core communication, for example [18] or Barrelfish UMP [5]. The basic idea is shown in Figure 3; to software, the sender writes data to a cache line on which the receiver is spinning (reading in a tight loop). Initially, the line is in (say) SHARED state in both caches. When the sender writes the line (typically in one go due to the core’s write-combining buffer), it transitions briefly to MODIFIED state, before being fetched by the receiver over the interconnect and reverting to SHARED.

This can be highly efficient in software, particularly when deployed as a ring buffer of cache lines, and results in very little interconnect traffic (since spinning is usually on a local copy of the line). One can easily replace one core with a device in this scheme (with suitable state machine) to obtain an I/O protocol. The downside is, of course, the CPU cost of spinning, both in wasted cycles and the inability to switch to another task.

The design of protocols like FastForward is based on the idea that each endpoint can only manipulate its local cache using software instructions: loads, stores, etc. Moreover, it is assumed (reasonably) that flush or invalidate instructions should be avoided because they might be slow, and might require kernel privilege.

This is not the case when one of the endpoints is a device with message-level access to the cache coherence protocol, and possibly maintaining its own directory state.

## 4.2 The implications of low-level access

Unlike software running on a core behind a cache, a device participating in a coherence protocol has visibility over more state and events, and can also initiate more operations. Note that there is no need for a cache *per se* on the device at all, indeed this is usually inappropriate.

First, the device **receives messages** from the CPU cache that request lines in SHARED or EXCLUSIVE state, or which request that the caching state on the be downgraded (e.g. from EXCLUSIVE to SHARED, or from SHARED to INVALID). It is therefore able to react internally to such events as it chooses, as long as it does not violate the protocol.

Second, the device can **issue such requests** itself at any time, allowing more fine-grained control of the state of a line in the CPU's cache.

Third, for lines which are homed at the device, the device' directory maintains explicit **information about the cache line state** at the CPU and other nodes as well as locally.

Fourth, unlike a conventional cache, the device **does not have to respond immediately** to every request from the CPU's cache. Instead, it can choose to delay the response (blocking the requesting core) until some other operations complete. Care must be taken to respond before any hardware-imposed timeouts, but these are typically generous (hundreds of milliseconds on the ThunderX-1, for example) and can be worked around in software (e.g. by sending a "try again" response within the timeout).

Finally, the device can **choose to interpret events** like remote requests as more than simply loads or stores to the line concerned. This last insight is important because it, in combination with the previous observation, it allows us to construct efficient communication mechanisms which rely on a combination of the device's richer view of the protocol and the software on the CPU adhering to additional conventions to communicate channel semantics to the device.

Put simply, requests to specific cache lines can be used to signal particular higher-level operations to the device, much as register reads and writes to traditional devices frequently have semantics very different from memory access.

This is an oversimplification, and we discuss the subtleties that arise below. First, however, we present four related communication protocols, layered above MESI-like coherence, which provide for efficient, blocking communication between a conventional CPU and a coherence-aware device.

## 4.3 Communication protocol variants

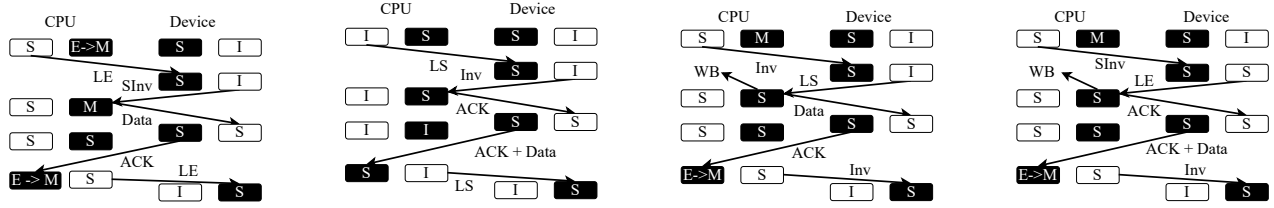
We present 4 different but similar communication protocols (shown in Figure 4) which vary based on (a) the CPU or the device initiates the message transfer, and (b) the cache lines used are homed on the CPU or device. All provide a synchronous RPC: a transfer of a single cache-line-sized message, followed by a single cache-line response. All use 2 cache lines, which we designate A and B. These protocols can be generalized to larger payloads, and latency will grow linearly with the payload size. Interestingly, they can be made slightly more efficient by using more cache lines, but quickly become complex. We focus on the simple 2-line case in this paper.

The protocols use the same techniques and insights, and are best described using the example of a CPU-initiated RPC using addresses homed on the device (Figure 4a). An implementation of this protocol is used for the evaluation in Section 5.1.

1. The protocol starts with line B in EXCLUSIVE state in the CPU cache, and line A INVALID. To initiate an operation, the CPU writes the request data from its registers into line B, which transitions to MODIFIED. This happens without communication with the device, since B was previously in EXCLUSIVE.
2. To signal to the device that line B holds a new request, the CPU then executes a load to line A. Since A is INVALID, the cache requests A in SHARED from the device. This violates the typical convention that cache line operations are independent, but the device is free to interpret this request for A as a signal from the CPU that B holds a request.
3. The device *does not respond* immediately to the request for A, thereby stalling the load and blocking the requesting core. Instead, it requests B from the CPU's cache, in EXCLUSIVE. The interconnect therefore transfers the request data to the device, and line B duly transitions to INVALID in the CPU's cache.
4. The device reads the data it has received in B, and computes a result on it, which is to be returned to the CPU. It returns this using the response to the CPU's request for cache line A.
5. The CPU cache receives line A's new data and the CPU unblocks, immediately loading the first word of the RPC response into a register.

As described, the resulting state is that A is now INVALID and B is SHARED in the CPU cache. However, in some deployed MESI-like protocols (including the Enzian interconnect we use), the device is free to return the data stipulating that it is not SHARED but now EXCLUSIVE to the CPU. This final feature leaves the cache in the state it started in, with the roles of A and B reversed, ready for the next transaction.

The whole exchange takes 2 round trips on the coherent interconnect.



(a) CPU-initiated, device-homed (b) Device-initiated and homed (c) CPU-initiated, CPU-homed (d) Dev.-initiated, CPU-homed

**Figure 4.** Protocol variants for efficient CPU-device messaging

The other 3 protocols work similarly. For example, [Figure 4b](#) shows the analogous case where the device initiates the request to the CPU, but still using lines homed on the device. This is used for the NIC experiment in [Section 5.3](#).

The remaining two cases, where the cache lines are homed on the CPU, are more complex to deal with, since there is a possibility that the CPU cache will evict one of the cache lines without warning. The device will not observe this, and so might incur an access to main memory on the CPU node. In this paper we therefore focus on the case where the cache lines are homed on the device.

#### 4.4 Discussion

A number of concerns might be raised about these protocols in practice; we address them in this section.

First is the issue of timeouts: we are blocking a core’s request for a cache line until a computation has completed. If this triggers a timeout in the CPU’s cache, the result is likely to be a memory fault exception, a machine check, or the processor simply locking up (on the Enzian, it is a machine check). We can work around these issues in practice by a small state machine on the device return a “not ready yet” response in the event of an approaching timeout, causing the software on the issue another request for the other cache line, extending the response time effectively indefinitely without the need for spinning. In practice, timeouts are quite long and the computations we target are short.

The second issue is more subtle, and concerns possible deadlock due to the device stalling a request until it can issue, and gets a reply back from, another to a different cache line. Such standards as exist for interoperable cache coherent interconnects are silent on what happens in this situation, possibly because it has not occurred until now. The design assumes that, in the platform, transactions on different cache lines can progress independently.

In most implementations, this assumption typically holds in order to maximize the memory bandwidth utilization and minimize request latency, and also to simplify reasoning about deadlock freedom of the coherence protocol itself. However, it may be the case that the cache stripes transactions across a limited number of independent units and

which might deadlock if both A and B were mapped to the same unit. Were this to be the case, it could be avoided by careful placement of A and B in the physical address space. This is actually the case in our FPGA device implementation, described in [Section 4.5](#).

#### 4.5 Implementation in Enzian

We implemented both device-homed protocols in the Enzian platform, which we use for the evaluation in [Section 5](#). The implementation uses SystemVerilog and exploits an existing “Directory Controller” on Enzian’s FPGA [\[42\]](#) which manages the coherent links to the CPU and handles transient states in the ECI protocol.

ECI provides all the messages we require to implement our messaging protocols. In particular, it includes the ability for the device to return a line to the CPU cache in EXCLUSIVE state, even though the CPU requested it in SHARED. This optimization (discussed in [Section 4.3](#)) dramatically reduces latency, as shown in [Section 5.1](#).

In our case, no flow-control issues arise since ECI uses separate virtual channels for request and reply messages, removing the chance of deadlock. However, other complications arise: ThunderX-1 generates Global Synchronization (GSYNC) messages which function as global barriers. A GSYNC blocks any subsequent transactions until all those started before the GSYNC have retired. But the invalidates sent are not awaited by the core they are still completed allowing the protocol to progress.

The ThunderX-1 divides its last-level cache functionality into a set of units called TADs, each of which can handle up to 16 simultaneous cache transactions. Two consecutive cache lines will be mapped to the different TADs by L2 to ensure that the operations can proceed independently.

On this CPU, barriers are needed to reliably order reads and writes. For example, it is critical that the core’s write buffer is drained into L1 cache (which is write-through to the L2) before a subsequent load from the core signals to the FPGA that the line can be pulled. The ARM architecture’s weak memory model requires a DMB barrier instruction between the writes and the read, and on the ThunderX-1 this is sufficient to ensure ordering observed at the FPGA.

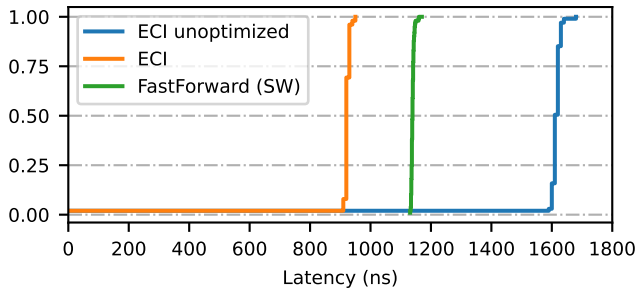


**Figure 5.** Round trip ECI RPC latency, plus software latency between two sockets

On the FPGA, control (interception) is performed based on AXI read requests, since both SHARED and EXCLUSIVE operations trigger these requests. The AXI writes go directly to the application. If the read is the result of the EXCLUSIVE, then the dummy data is sent back to the CPU as here is no fresh result yet.

## 5 Evaluation

In this section, we compare PIO over a coherent interconnect with two other reference points: PIO directly over PCIe – essentially, the CPU copying data to and from a region of PCIe address space – and descriptor-based DMA over PCIe. All use the same Enzian hardware platform. Coherent PIO uses the Enzian native ECI, while the two PCIe techniques connect the CPU and FPGA PCIe interfaces back-to-back with a loopback cable as described in Section 3, effectively turning the Enzian FPGA into a conventional PCIe FPGA card. DMA experiments all use the Xilinx XDMA hardware IP on the FPGA.

We explore three different application scenarios: synchronous RPC to an accelerator on the FPGA, a closely-coupled high-speed NIC, and a stream processor which moves some of its dataflow operator graph to the FPGA.

### 5.1 RPC to an accelerator

The first experiment measures null-RPC latency when the CPU invokes a function on the device, passing arguments, and obtaining a result. The protocol shown in Figure 4a and detailed in Section 4.3 is used (i.e. the cache lines used for communication are homed on the FPGA).

Figure 5 shows the distribution of total latency for the this operation. We see a median latency of around 1600ns for the *unoptimized* protocol, wherein the result line is returned in SHARED state as it was requested by the CPU. When we introduce the optimization of returning the line in EXCLUSIVE, the median latency drops to around 900ns.

For comparison, we also show an implementation of the FastForward protocol [18] exchanging cache lines between

```

1 // map 4KiB of PCIe memory for read/write
2 int fd = open("/sys/bus/pci/devices/.../resource0",
3             O_RDWR);
4 void *pcie_bar = mmap(NULL, 4096,
5                       PROT_READ | PROT_WRITE, MAP_SHARED, fd, 0);
6
7 // write RPC arguments to PCIe memory
8 *(volatile rpc_args_t *)pcie_bar = rpc_args;
9 __sync_synchronize();
10
11 // read RPC result from PCIe memory
12 rpc_res_t rpc_res = *(volatile rpc_res_t *)pcie_bar;
13 __sync_synchronize();

```

**Listing 1.** Example RPC using PIO over PCIe on Linux. Error handling not shown for brevity.

sockets in a dual-socket ThunderX-1-based Gigabyte R150-T61 server with similar CPU and DDR specification to Enzian; this achieves a median latency of about 1150ns.

The optimized protocol is performing 2 round-trip message exchanges over ECI, which has a one-way latency at the link later of about 150ns. The rest of the overhead (300ns) is mostly incurred in the protocol processing in the directory controller. The FPGA is clocked at about 300MHz.

A significant penalty is incurred when the results of the RPC are returned in SHARED, resulting in further round trips over ECI to (unnecessarily) invalidate the line at the FPGA before sending the next message. This suggests that future coherent interconnects would benefit greatly from allowing this kind of operation.

Overall, the optimized protocol comfortably outperforms FastForward, despite the latter exploiting highly optimized hardware implementations at both ends (clocked at 2.1GHz) and aggressively polling, whereas our optimized protocol requires no spinning on the part of the CPU or device.

### 5.2 RPC over ECI vs. PCIe PIO and DMA

We now compare the RPC latency achieved using our protocol over ECI with PIO over PCIe and the Xilinx XDMA hardware using descriptors.

For PIO over PCIe we pre-map the relevant PCIe aperture (BAR) into user space on the CPU and measure the time to write a value to this space and read a result back, as illustrated in Listing 1. For XDMA numbers we use Xilinx XDMA benchmark [51], which essentially performs the same operation using descriptor-based DMA. In both these cases, the FPGA is configured to map the request and response into a write to and a read from onboard Block RAM, respectively.

As in Section 5.1, we measure latency to send a request from the CPU to the FPGA and read a response. However, this

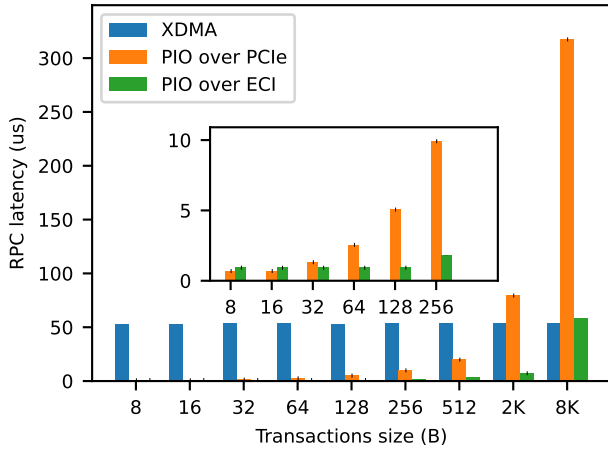


Figure 6. RPC latency for different payload sizes

time we vary the payload size (of both request and response) and report median latency figures.

The results are shown in Figure 6. Up to payloads of 8KiB, the latency of XMDA-based communication is completely dominated by descriptor setup and manipulation, and remains largely independent of payload size. Faster PCIe interconnects \*recall that this is a PCIe Gen3 x8 link) would only further emphasize this.

Latency over ECI is dramatically lower for smaller payloads. Unsurprisingly, it is constant up to 128 bytes (the size of a cache line on Enzian) and then increases linearly, since the protocol simply replicates each cache line exchange until all the data has been transferred. It is only at 8KiB that ECI RPC latency exceeds that of XMDA. One might argue that the transfer of multiple cache lines over ECI might be improved by clever pipelining and locating the lines in physical memory so as to exploit parallelism in the directory controllers, but we do not explore that in this paper.

Relative to ECI, PIO over PCIe performs poorly except for payloads under 16 bytes in size. As we show in Section 5.3, this is because PCIe memory reads are *non-posted* transactions, forcing a read to finish before the next can be issued and potentially incurring a round trip time penalty (about  $1\mu\text{s}$ ) for each word transferred. Moreover, many systems have a narrow read bus between CPU and PCIe: for example, the ThunderX-1 peripheral access bus is only 128 bits wide. In comparison, memory writes on PCIe are *posted* transactions and may complete out of order. Most systems (including ThunderX-1) have dedicated bus units to combine writes and coalesce PCIe transactions.

On this platform, using common techniques to improve performance like vector instructions has limited or no benefit for PIO over PCIe. For writes, the hardware already performs coalescing, and we see transactions of up to 512 bits regardless of vector size (confirmed using a logic analyzer). For

reads, the 128 bit limit remains, and is responsible for the increase in latency between 16-byte and 32-byte payloads.

We conclude that up to the page size (4KiB) or the typical size of jumbo frames, PIO remains significantly faster than the DMA option commonly used for these transaction sizes. Thus even using the XDMA implementation for the experiments we still have the room for comparison with optimized DMA implementations.

### 5.3 Network interface

We now compare the different approaches in the context of data center networking. It is not uncommon to see very low latency figures ( $< 1\mu\text{s}$ ) in data center packet switching and delivery [20, 22, 27], motivating the need to minimize latency between the network itself and CPU registers [17].

We implement 3 variations of a 100Gb/s NIC on Enzian. The first (Figure 7a) is a conventional approach connecting one of Enzian’s 100Gb Ethernet MACs fairly directly to the XDMA engines, resulting in a NIC which is programmed using descriptor rings. The second design (Figure 7b) buffers packets in onboard SRAM on the FPGA and allows the CPU to read and write packet and control data using PCIe reads and writes. The final approach (Figure 7c) uses a custom module on the FPGA to bridge between the ECI directory controller and the Ethernet MAC, using the protocol in Figure 4b to deliver network packets to the CPU in cache lines. In all cases we clock the core NIC logic at 250 MHz.

For experiments we configure the Ethernet MAC in near-end PCS/PMA loopback mode for a reliable measurement of packet delivery *inside* the server without network delays. We define the receive latency as time passed from the last beat of the packet appearing on the ingress streaming interface of the Ethernet MAC, to the CPU fully receiving the packet content in its registers. The transmit latency is defined similarly as time passed from the CPU having the packet ready in registers, to the last beat of the packet appearing on the egress streaming interface on the MAC. We do not include the time it takes the packet to go through the Ethernet PCS/PMA loopback, since the MAC is fixed and the same in all implementations presented in this experiment.

We show figures for XDMA in both polled and interrupt-driven modes; in practice the difference in latency is small.

Figure 8 shows receive latency for different packet sizes for each of the NIC implementations. As in the RPC experiment, DMA latency is fairly stable across all packet sizes, suggesting that the latency is dominated by various DMA overheads, such as descriptor setup and manipulation.

Note that system calls here actually result in very little overhead (only a few microseconds); the overhead is actually dominated by cache misses manipulating DMA data structures in main memory.



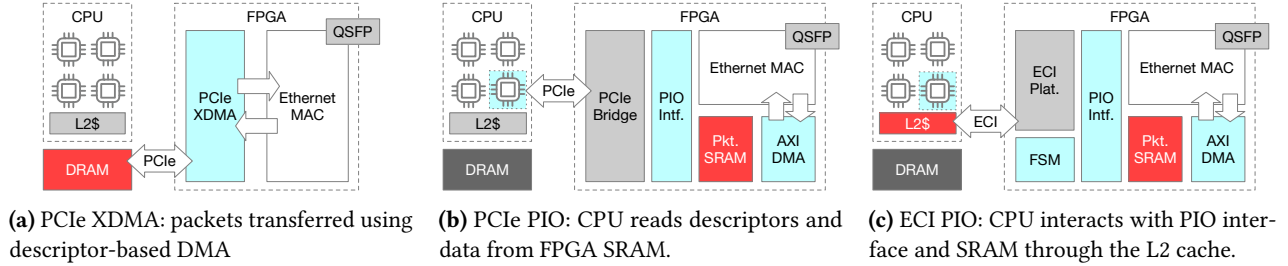


**Figure 7.** Different NIC architectures. Blue denotes data movers; red denotes memory that holds packet data.

In contrary, PIO over both ECI and PCIe offer much lower latency for small packet sizes up to 1024 bytes DMA, highlighting high efficiency gains in PIO compared to DMA. However, the latency of PCIe PIO quickly degrades for larger packets due to the “non-posted read” problem discussed in Section 5.2, reaching over  $350\mu\text{s}$  for 8KiB packets. In contrast, ECI offers dramatically better latency even at 8KiB packets.

Figure 9 shows transmit latency. In this case, PCIe PIO competes well with ECI across all packet sizes due to combining posted writes. PIO over ECI shows a slightly higher latency for small packets, due to it needing 2 round-trips over ECI for each 128 bytes, versus a single PCIe round trip. Both PIO solutions perform significantly better than DMA across all packet sizes.

These results show a clear advantage of using PIO over DMA, even for larger packets. The poor receive performance of PCIe-based PIO for receiving packets is largely due to a limitation of the PCIe design, that disappears for transmit.

#### 5.4 Worked Example: Offloading Timely Dataflow

In this example we apply the techniques and results outlined so far to a practical workload: Timely Dataflow [48], a real-time stream-processing system. We compare the baseline performance to a partially FPGA-offloaded implementation under three CPU–FPGA communication scenarios: DMA over PCIe, PIO over PCIe, and PIO over ECI.

Timely Dataflow schedules operators in a user-defined dataflow graph to evaluate complex operations on large streams of data, operating on variable-sized batches. Operators may be arbitrarily complex and are independent, and thus benefit from offloading where the overhead of shipping the data to the FPGA is compensated by greater throughput of the offloaded operators.

To test the limits, we construct a worst-case scenario: a large (31-element) graph of simple operators (filters). The large graph maximizes communication overhead in the form of progress tracking data, while the simple operators leave the FPGA with only a small performance lead over the CPU. We want to predict whether PIO can make FPGA offload work in regimes where the fixed overheads of DMA make it impractical, for example where small batch sizes are needed to ensure data freshness (as in Differential Dataflow).

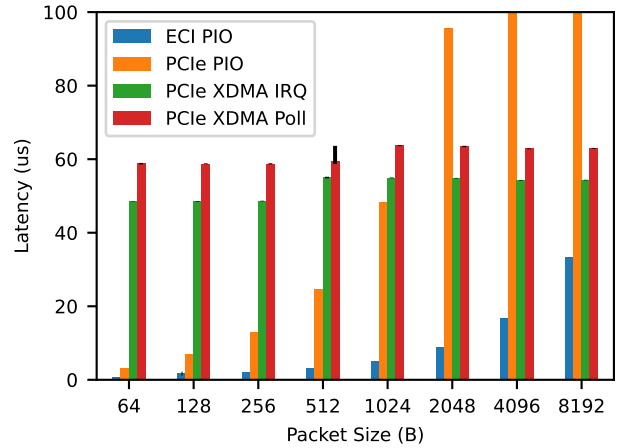


**Figure 8.** NIC implementations: receive latency

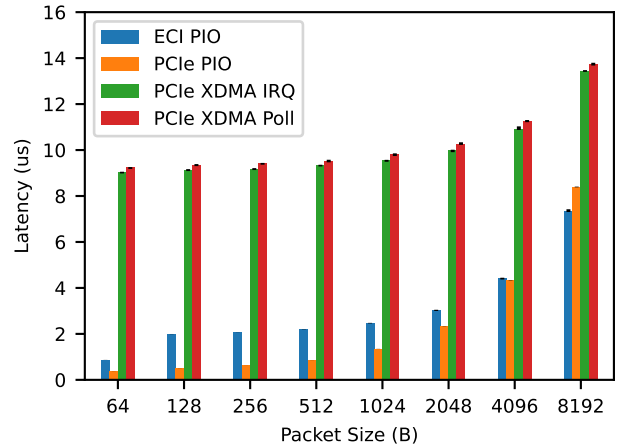


**Figure 9.** NIC implementations: transmit latency

The first (blue) bars of Figure 10 show the baseline performance of the non-offloaded (CPU-only) system against batch size. Note that the horizontal axis is a log scale; All four curves are actually straight lines, with offsets and slopes obtained by a least-squares fit listed in Table 1 along with the

coefficient of determination ( $r^2$ ). The remaining bars cover the three offload cases. Each is the median of 1000 samples.

While no offload configuration beats the baseline, the two PIO cases outperform DMA up to batch sizes of 512B (for PCIe) and 4KiB (for ECI), with ECI almost matching the baseline at the smallest batch size (128B). To understand why offloading fails to produce a speedup in this example, and what changes will be necessary to allow it to, we look more closely at the fitted coefficients in Table 1.

As shown by the  $r^2$  values, the fit for each dataset is excellent. We can thus model the time taken to process a batch as a fixed component, or overhead, independent of the amount of data processed (e.g. running the Timely scheduler, or setting up DMA descriptors) plus a component which scales linearly with the size of the batch.

Compared to the baseline, DMA offload has a significantly lower per-byte cost (3.7 vs. 8.7ns/B) but higher fixed cost (336 $\mu$ s vs. 204 $\mu$ s). This includes the cost of descriptor setup and interrupt handling, while the per-byte cost shows the higher throughput of the FPGA. This includes both computation and data transfer but as DMA makes very efficient use of the (PCIe 3.0 x8) interconnect, once setup costs are paid, the per-byte transfer cost is on the order of 0.1ns, allowing us to estimate the per-byte cost of FPGA compute at 3.6ns/B. The CPU figure represents only compute.

This linear model predicts a break-even at 26KiB. This matches the observed data (not plotted) where DMA offload first outperforms the baseline at a batch size of 32KiB. Whenever the FPGA compute cost is at least 0.1ns lower per byte than the CPU, DMA offload will outperform for large enough batches. However, due to the large fixed overhead it can never outperform the CPU for batches smaller than 16KiB. This limits its usefulness where small batch sizes are needed.

While they make less efficient use of the interconnect bandwidth (as indicated by their higher per-byte costs), their lower fixed overhead allows the PIO modes to significantly outperform DMA at smaller batch sizes. What would it take for the faster of the two (ECI) to outperform the CPU at a moderate batch size?

As the FPGA pipeline is identical in all cases, the limiting factor is the per-byte transfer cost. Taking our above estimate of FPGA compute at 3.6ns/B, we can estimate this cost at  $30 - 3.6 = 26.4ns/B$ . Letting  $S$  stand for batch size and  $C$  for this transfer cost, the two break even where

$$204\mu s + S \times 8.7ns/B = 221\mu s + S \times (C + 3.6ns/B)$$

Rearranging gives

$$C = 5.1ns/B - 17\mu s/S$$

5.1ns/B being the speedup due to FPGA processing and 17 $\mu$ s the fixed overhead relative the baseline, the negative sign due to the higher-than-baseline overhead.

From this we see that given the overhead the smallest batch for which a speedup is possible is around 3300B, and

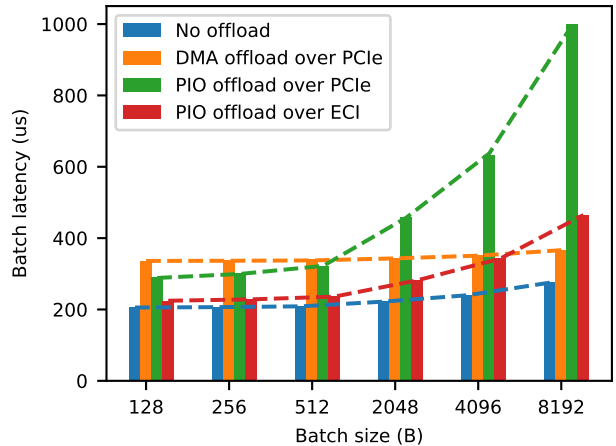


**Figure 10.** DMA and PIO performance for Timely Dataflow FPGA offload with a graph size 31

	time/byte (ns)	overhead ( $\mu$ s)	$r^2$
Baseline	8.7	204	1.00
PCIe-DMA	3.7	336	0.99
PCIe-PIO	88	277	1.00
ECI-PIO	30	221	1.00

**Table 1.** 1st-order (offset + slope) coefficients fitted to the data series of Figure 10, as cost per byte and fixed overhead

that a batch size of 4096B demands a transfer cost not more than 0.95ns/B, or 120ns per 128B cache line. As the existing protocol serializes on each line, this cost includes the round-trip latency. As the hardware can handle many in-flight transfers at once, modifying the protocol to transfer 32 lines at once would reduce the per-byte cost enough that ECI-PIO offload breaks even.

Alternatively or additionally, bringing the fixed cost down reduces the smallest practical batch. If the relative overhead could be brought below 500ns/batch then with parallel cache lines giving a 1ns/B transfer cost, FPGA offload using ECI-PIO would outperform the CPU from a batch size of 128B, or a single cache line. With such an optimized protocol, ECI-PIO would outperform all other cases until a batch size of 142KiB, above which PCIe-DMA would overtake it giving a net offload benefit across all batch sizes.

## 6 Related work

### 6.1 Coherent interconnects

Coherent replacements or extensions of existing device interconnects have been under development for some time and are beginning to see widespread availability. IBM’s OpenCAPI [45] builds on PCIe by adding a protocol layer for coherence. It and the competing Gen-Z [31] and CCIX [11]

protocols have meanwhile been either merged into or replaced by CXL [34], which seems likely to be the standard interoperable protocol in the short- to medium-term future.

Commercial CXL hardware implementing the more recent revisions, which allow less restricted use cases, is still not widely available. Consequently research on the software uses of coherent interconnects is still largely performed on specifically research-oriented machines such as the Intel HARP [24, 25], and Enzian [13]. While HARP provides a pre-configured coherent cache in the FPGA with a conventional interface, Enzian’s ECI protocol is fully open and customizable.

Other notable coherent interconnects include the RISC-V-specific TileLink [8, 14, 47] and NVIDIA’s NVLink 2.0 [39, 50]. TileLink is an open standard and suitable for research but hasn’t yet been implemented in server-scale hardware. NVLink is proprietary and closed.

Existing work has built on the available research platforms to explore the design space for practical applications. Centaur [41] demonstrated the FPGA offload of database operations on Intel HARP v1, and Cohort [36, 49] proposed and prototyped a unified queue-based software interface to such accelerators building on the P-Mesh interconnect of OpenPiton [40].

Open, extensible protocols have been used to explore coherent offload in simulation, including making the case for protocol specialization building on the Spandex protocol family [2, 3]. Conda [9] likewise employed simulation to explore the design space for coherent device interconnects, with a focus on reducing unnecessary message traffic.

The Denovo protocol [44] is presented as an improvement specifically for CPU-GPU coherence, tailoring the protocol to match the comparatively predictable access patterns of typical GPU workloads.

## 6.2 Cache line-based communication

Other work [46] has already noted that the cache line is a better unit of transfer where small operations are expected. This is a common observation, long since applied in the original FastForward [19] and Barrelfish UMP [6] protocols. More recently Concord [26] communicates scheduling decisions between workers and the dispatcher via a polled cache line, converting worker threads from interrupt-driven to poll-mode “CPU drivers”. A similar technique is used in Shinjuku [28].

A recent study of data center RPC from Google [29] reinforces the importance of small transfers and highlights the large latency of PCIe transactions.

## 6.3 Exploring PIO

The space where PIO is preferable to DMA is likewise well studied. The hXDP [10] FPGA NIC work highlighted the high overhead of small PCIe transactions, and consequently performs small batch computations solely on the CPU.

In kPIO+WC [32] the authors demonstrate the benefit of write combining for PCIe-based PIO. Compared to a traditional DMA NIC, their FPGA-based prototype shows better latency and throughput for small and medium-sized messages and comparable throughput for large messages. The ThunderX CPU automatically performs combining for PCIe writes, and the results of Section 5.2 thus reflect this optimization.

Neugebauer et. al. [38] provide a comprehensive analysis of PCIe performance in the context of NICs.

Dagger [33] builds on CCI-P, the commercialized implementation of HARP’s coherent cache, to construct an FPGA-based NIC specialized for low latency RPC. A host-coherent cache holds connection states and the necessary structures for the transport layer on the NIC, while the payload remains in host memory. This minimizes FPGA memory demands, and exploits the lower latency of cache misses compared to conventional PCIe-based NICs.

## 7 Conclusion and Future Work

In this paper we have demonstrated that PIO on modern hardware outperforms DMA over a wide range of payload sizes in a number of different applications. For anything up to a disk block, VM page, or Ethernet Jumbo Frame, PIO offers (often dramatically) lower transfer times mostly thanks to its low fixed overheads. This advantage is consistent across RPC workloads, NIC packet transfer, and FPGA offloaded applications.

This strongly contradicts the accepted wisdom, under which these specific payloads and applications are the canonical examples of DMA-suitable tasks. Moving beyond conventional interconnects (PCIe), we have shown that the advantage grows even greater for the emerging class of coherent interconnects. This is partly due to a more suitably-sized unit of transfer (the cache line) and partly due to the opportunity to interact with the coherence protocol in a carefully-optimized manner.

Moving back to PIO makes sense in a landscape of plentiful, cheap CPU cores and fine-grained RPC-style workloads.

This work is ongoing, and we intend to develop it further in several ways. Both the cache-coherent NIC and Timely Dataflow offload designs will continue to be optimized, to explore the limits of PIO-style device communication on emerging coherent interconnects. We will also further explore the design of appropriate programming interfaces and OS-level integration of coherent mechanisms for high-performance devices.

## References

- [1] Brian Allison, Michael Siegel, and Rick Hagen. 2020. OpenCAPI Transaction Layer Specification. (2020).
- [2] Johnathan Alsop, Weon Taek Na, Matthew D. Sinclair, Samuel Grayson, and Sarita Adve. 2022. A Case for Fine-grain Coherence Specialization in Heterogeneous Systems. *ACM Trans. Archit. Code Optim.* 19, 3,

- Article 41 (aug 2022), 26 pages. <https://doi.org/10.1145/3530819>
- [3] Johnathan Alsop, Matthew D. Sinclair, and Sarita V. Adve. 2018. Span-  
dex: a flexible interface for efficient heterogeneous coherence. In *Proceedings of the 45th Annual International Symposium on Computer Architecture* (Los Angeles, California) (ISCA '18). IEEE Press, 261–274. <https://doi.org/10.1109/ISCA.2018.00031>
  - [4] AMBA® CHI Architecture Specification 2024. <https://developer.arm.com/documentation/ih0050/latest/>
  - [5] Andrew Baumann, Paul Barham, Pierre-Evariste Dagand, Tim Harris, Rebecca Isaacs, Simon Peter, Timothy Roscoe, Adrian Schüpbach, and Akhilesh Singhanian. 2009. The Multikernel: a new OS architecture for scalable multicore systems. In *Proceedings of the ACM SIGOPS 22nd Symposium on Operating Systems Principles* (Big Sky, Montana, USA) (SOSP '09). Association for Computing Machinery, New York, NY, USA, 29–44. <https://doi.org/10.1145/1629575.1629579>
  - [6] Andrew Baumann, Paul Barham, Pierre-Evariste Dagand, Tim Harris, Rebecca Isaacs, Simon Peter, Timothy Roscoe, Adrian Schüpbach, and Akhilesh Singhanian. 2009. The Multikernel: A New OS Architecture for Scalable Multicore Systems. In *Proceedings of the ACM SIGOPS 22nd Symposium on Operating Systems Principles* (Big Sky, Montana, USA) (SOSP '09). ACM, New York, NY, USA, 29–44. <https://doi.org/10.1145/1629575.1629579>
  - [7] Andrew Bean. 2016. Improving memory access performance for irregular algorithms in heterogeneous CPU/FPGA systems. (Jan. 2016). <https://doi.org/10.25560/41981> Accepted: 2016-10-25T15:31:13Z Publisher: Imperial College London.
  - [8] Berkeley Architecture Research. 2022. TileLink. <https://bar.eecs.berkeley.edu/projects/tilelink.html>
  - [9] Amirali Boroumand, Saugata Ghose, Minesh Patel, Hasan Hassan, Brandon Lucia, Rachata Ausavarungnirun, Kevin Hsieh, Nastaran Hajinazar, Krishna T. Malladi, Hongzhong Zheng, and Onur Mutlu. 2019. CoNDA: Efficient Cache Coherence Support for near-Data Accelerators. In *Proceedings of the 46th International Symposium on Computer Architecture*. 629–642.
  - [10] Marco Spaziani Brunella, Giacomo Belocchi, Marco Bonola, Salvatore Pontarelli, Giuseppe Siracusano, Giuseppe Bianchi, Aniello Cammarano, Alessandro Palumbo, Luca Petrucci, and Roberto Bifulco. 2020. hXDP: Efficient Software Packet Processing on FPGA NICs. In *14th USENIX Symposium on Operating Systems Design and Implementation (OSDI 20)*. USENIX Association, 973–990. <https://www.usenix.org/conference/osdi20/presentation/brunella>
  - [11] CCIX Consortium and others. 2024. Cache Coherent Interconnect for Accelerators (CCIX). <http://www.ccixconsortium.com>
  - [12] Mahesh Chaudhari, Kedar Kulkarni, Shreeya Badhe, and Vandana In-  
amdar. 2017. Evaluating Effect of Write Combining on PCIe Through-  
put to Improve HPC Interconnect Performance. In *2017 IEEE International Conference on Cluster Computing (CLUSTER)*. IEEE, Honolulu, HI, USA, 639–640. <https://doi.org/10.1109/CLUSTER.2017.109>
  - [13] David Cock, Abishek Ramdas, Daniel Schwyn, Michael Giardino, Adam Turowski, Zhenhao He, Nora Hossle, Dario Korolija, Melissa Licciardello, Kristina Martsenko, Reto Acherhmann, Gustavo Alonso, and Timothy Roscoe. 2022. Enzian: an open, general CPU/FPGA platform for systems software research. In *Proceedings of the 27th ACM International Conference on Architectural Support for Programming Languages and Operating Systems* (Lausanne, Switzerland) (ASPLOS 2022). Association for Computing Machinery, New York, NY, USA, 590–607. <https://doi.org/10.1145/3503222.3507742>
  - [14] Henry Cook, Wesley Terpstra, and Yunsup Lee. 2017. Diplomatic Design Patterns: A TileLink Case Study. In *First Workshop on Computer Architecture Research with RISC-V (CARRV 2017)*.
  - [15] CXL Consortium. 2024. Compute Express Link. [https://computeexpresslink.org/wp-content/uploads/2023/12/CXL\\_3\\_0\\_white-paper\\_FINAL.pdf](https://computeexpresslink.org/wp-content/uploads/2023/12/CXL_3_0_white-paper_FINAL.pdf)
  - [16] CXL Consortium. 2024. Compute Express Link. <https://www.computeexpresslink.org/>
  - [17] Geetanjali Gadre, Shreeya Badhe, and Kedar Kulkarni. 2016. Network processor—A simplified approach for transport layer offloading on NIC. In *2016 International Conference on Advances in Computing, Communications and Informatics (ICACCI)*. IEEE, Jaipur, India, 2542–2548. <https://doi.org/10.1109/ICACCI.2016.7732440>
  - [18] John Giacomoni, Tipp Moseley, and Manish Vachharajani. 2008. Fast-Forward for efficient pipeline parallelism: a cache-optimized concurrent lock-free queue. In *Proceedings of the 13th ACM SIGPLAN Symposium on Principles and Practice of Parallel Programming* (Salt Lake City, UT, USA) (PPoPP '08). Association for Computing Machinery, New York, NY, USA, 43–52. <https://doi.org/10.1145/1345206.1345215>
  - [19] John Giacomoni, Tipp Moseley, and Manish Vachharajani. 2008. Fast-Forward for Efficient Pipeline Parallelism: A Cache-Optimized Concurrent Lock-Free Queue. In *Proceedings of the 13th ACM SIGPLAN Symposium on Principles and Practice of Parallel Programming* (Salt Lake City, UT, USA) (PPoPP '08). Association for Computing Machinery, New York, NY, USA, 43–52. <https://doi.org/10.1145/1345206.1345215>
  - [20] Dan Gibson, Hema Hariharan, Eric Lance, Moray McLaren, Behnam Montazeri, Arjun Singh, Stephen Wang, Hassan M. G. Wassel, Zhehua Wu, Sunghwan Yoo, Raghuraman Balasubramanian, Prashant Chandra, Michael Cutforth, Peter Cuy, David Decotigny, Rakesh Gautam, Alex Iriza, Milo M. K. Martin, Rick Roy, Zuowei Shen, Ming Tan, Ye Tang, Monica Wong-Chan, Joe Zbiciak, and Amin Vahdat. 2022. Aquila: A unified, low-latency fabric for datacenter networks. 1249–1266. <https://www.usenix.org/conference/nsdi22/presentation/gibson>
  - [21] Roberto Gioiosa, Thomas Warfel, Antonino Tumeo, and Ryan Friese. 2017. Pushing the Limits of Irregular Access Patterns on Emerging Network Architecture: A Case Study. In *2017 IEEE International Conference on Cluster Computing (CLUSTER)*. IEEE, Honolulu, HI, USA, 874–881. <https://doi.org/10.1109/CLUSTER.2017.125>
  - [22] Mark Handley, Costin Raiciu, Alexandru Agache, Andrei Voinescu, Andrew W. Moore, Gianni Antichi, and Marcin WĄjcik. 2017. Researching datacenter networks and stacks for low latency and high performance. In *Proceedings of the Conference of the ACM Special Interest Group on Data Communication*. ACM, Los Angeles CA USA, 29–42. <https://doi.org/10.1145/3098822.3098825>
  - [23] Sara Hooker. 2021. The hardware lottery. *Commun. ACM* 64, 12 (Dec. 2021), 58–65. <https://doi.org/10.1145/3467017>
  - [24] Intel. 2024. Intel Acceleration Stack for Intel® Xeon® CPU with FPGAs Core Cache Interface (CCI-P). <https://www.intel.com/content/www/us/en/docs/programmable/683193/current/acceleration-stack-for-cpu-with-fpgas.html>
  - [25] Intel Harp. 2024. IvyTown Xeon + FPGA: The HARP Program. [https://cpufpga.wordpress.com/wp-content/uploads/2016/04/harp\\_isca\\_2016\\_final.pdf](https://cpufpga.wordpress.com/wp-content/uploads/2016/04/harp_isca_2016_final.pdf)
  - [26] Rishabh Iyer, Musa Unal, Marios Kogias, and George Candea. 2023. Achieving Microsecond-Scale Tail Latency Efficiently with Approximate Optimal Scheduling. In *Proceedings of the 29th Symposium on Operating Systems Principles* (<conf-loc>, <city>Koblenz</city>, <country>Germany</country>, </conf-loc>) (SOSP '23). Association for Computing Machinery, New York, NY, USA, 466–481. <https://doi.org/10.1145/3600006.3613136>
  - [27] Christoforos Kachris, Konstantinos Kanonakis, and Ioannis Tomkos. 2013. Optical interconnection networks in data centers: recent trends and future challenges. *IEEE Communications Magazine* 51, 9 (Sept. 2013), 39–45. <https://doi.org/10.1109/MCOM.2013.6588648>
  - [28] Kostis Kaffes, Timothy Chong, Jack Tigar Humphries, Adam Belay, David Mazières, and Christos Kozyrakis. 2019. Shinjuku: Preemptive Scheduling for msecond-scale Tail Latency. In *16th USENIX Symposium on Networked Systems Design and Implementation (NSDI 19)*. USENIX Association, Boston, MA, 345–360. <https://www.usenix.org/conference/nsdi19/presentation/kaffes>

- [29] Sagar Karandikar, Chris Leary, Chris Kennelly, Jerry Zhao, Dinesh Parimi, Borivoje Nikolic, Krste Asanovic, and Parthasarathy Ranganathan. 2021. A Hardware Accelerator for Protocol Buffers. In *MICRO-54: 54th Annual IEEE/ACM International Symposium on Microarchitecture* (Virtual Event, Greece) (*MICRO '21*). Association for Computing Machinery, New York, NY, USA, 462–478. <https://doi.org/10.1145/3466752.3480051>
- [30] Tomoya Kashimata, Toshiaki Kitamura, Keiji Kimura, and Hironori Kasahara. 2019. Cascaded DMA Controller for Speedup of Indirect Memory Access in Irregular Applications. In *2019 IEEE/ACM 9th Workshop on Irregular Applications: Architectures and Algorithms (IA3)*. IEEE, Denver, CO, USA, 71–76. <https://doi.org/10.1109/IA349570.2019.00017>
- [31] Kimberly Keeton. 2015. The Machine: An Architecture for Memory-centric Computing. In *Proceedings of the 5th International Workshop on Runtime and Operating Systems for Supercomputers*. ACM, Portland OR USA, 1–1. <https://doi.org/10.1145/2768405.2768406>
- [32] Steen Larsen and Ben Lee. 2015. Reevaluation of programmed I/O with write-combining buffers to improve I/O performance on cluster systems. In *2015 IEEE International Conference on Networking, Architecture and Storage (NAS)*. IEEE, Boston, MA, USA, 345–346. <https://doi.org/10.1109/NAS.2015.7255219>
- [33] Nikita Lazarev, Shaojie Xiang, Neil Adit, Zhiru Zhang, and Christina Delimitrou. 2021. Dagger: efficient and fast RPCs in cloud microservices with near-memory reconfigurable NICs. In *Proceedings of the 26th ACM International Conference on Architectural Support for Programming Languages and Operating Systems (Virtual, USA) (ASPLOS '21)*. Association for Computing Machinery, New York, NY, USA, 36–51. <https://doi.org/10.1145/3445814.3446696>
- [34] Huaicheng Li, Daniel S. Berger, Lisa Hsu, Daniel Ernst, Pantea Zardoshti, Stanko Novakovic, Monish Shah, Samir Rajadnya, Scott Lee, Ishwar Agarwal, Mark D. Hill, Marcus Fontoura, and Ricardo Bianchini. 2023. Pond: CXL-Based Memory Pooling Systems for Cloud Platforms. In *Proceedings of the 28th ACM International Conference on Architectural Support for Programming Languages and Operating Systems, Volume 2* (Vancouver, BC, Canada) (*ASPLOS 2023*). Association for Computing Machinery, New York, NY, USA, 574–587. <https://doi.org/10.1145/3575693.3578835>
- [35] Michael Marty, Marc de Kruijf, Jacob Adriaens, Christopher Alfeld, Sean Bauer, Carlo Contavalli, Michael Dalton, Nandita Dukkupati, William C. Evans, Steve Gribble, Nicholas Kidd, Roman Kononov, Gautam Kumar, Carl Mauer, Emily Musick, Lena Olson, Erik Rubow, Michael Ryan, Kevin Springborn, Paul Turner, Valas Valancius, Xi Wang, and Amin Vahdat. 2019. Snap: a microkernel approach to host networking. In *Proceedings of the 27th ACM Symposium on Operating Systems Principles* (Huntsville, Ontario, Canada) (*SOSP '19*). Association for Computing Machinery, New York, NY, USA, 399–413. <https://doi.org/10.1145/3341301.3359657>
- [36] Shubhendu S. Mukherjee, Babak Falsafi, Mark D. Hill, and David A. Wood. 1996. Coherent network interfaces for fine-grain communication. *SIGARCH Comput. Archit. News* 24, 2 (may 1996), 247–258. <https://doi.org/10.1145/232974.232999>
- [37] Vijay Nagarajan, Daniel J. Sorin, Mark D. Hill, and David A. Wood. 2020. *A Primer on Memory Consistency and Cache Coherence: Second Edition*. Morgan and Claypool.
- [38] Rolf Neugebauer, Gianni Antichi, José Fernando Zazo, Yury Audzevich, Sergio López-Buedo, and Andrew W. Moore. 2018. Understanding PCIe performance for end host networking. In *Proceedings of the 2018 Conference of the ACM Special Interest Group on Data Communication* (Budapest, Hungary) (*SIGCOMM '18*). Association for Computing Machinery, New York, NY, USA, 327–341. <https://doi.org/10.1145/3230543.3230560>
- [39] Nvidia. 2024. NVLink. <https://www.nvidia.com/en-us/data-center/nvlink/>
- [40] OpenPiton Open Source Research Processor 2024. <https://parallel.princeton.edu/openpiton/>
- [41] Muhsen Owaida, David Sidler, Kaan Kara, and Gustavo Alonso. 2017. Centaur: A Framework for Hybrid CPU-FPGA Databases. In *2017 IEEE 25th Annual International Symposium on Field-Programmable Custom Computing Machines (FCCM)*. 211–218. <https://doi.org/10.1109/FCCM.2017.37>
- [42] Abishek Ramdas. 2024. CCKit: FPGA acceleration in symmetric coherent heterogeneous platforms. [https://www.research-collection.ethz.ch/bitstream/handle/20.500.11850/642567/Thesis\\_AR.pdf?sequence=1&isAllowed=y](https://www.research-collection.ethz.ch/bitstream/handle/20.500.11850/642567/Thesis_AR.pdf?sequence=1&isAllowed=y)
- [43] Henry N. Schuh, Arvind Krishnamurthy, David Culler, Henry M. Levy, Luigi Rizzo, Samira Khan, and Brent E. Stephens. 2024. CC-NIC: a Cache-Coherent Interface to the NIC. In *Proceedings of the 29th ACM International Conference on Architectural Support for Programming Languages and Operating Systems, Volume 1* (La Jolla, CA, USA) (*ASPLOS '24*). Association for Computing Machinery, New York, NY, USA, 52–68. <https://doi.org/10.1145/3617232.3624868>
- [44] Matthew D. Sinclair, Johnathan Alsop, and Sarita V. Adve. 2015. Efficient GPU synchronization without scopes: Saying no to complex consistency models. In *2015 48th Annual IEEE/ACM International Symposium on Microarchitecture (MICRO)*. 647–659. <https://doi.org/10.1145/2830772.2830821>
- [45] J. Stuecheli, W. J. Starke, J. D. Irish, L. B. Arimilli, D. Dreps, B. Blaner, C. Wollbrink, and B. Allison. 2018. IBM POWER9 opens up a new era of acceleration enablement: OpenCAPI. *IBM Journal of Research and Development* 62, 4/5 (2018), 8:1–8:8. <https://doi.org/10.1147/JRD.2018.2856978>
- [46] Sajjad Tamimi, Florian Stock, Andreas Koch, Arthur Bernhardt, and Iliia Petrov. 2022. An Evaluation of Using CCIX for Cache-Coherent Host-FPGA Interfacing. In *2022 IEEE 30th Annual International Symposium on Field-Programmable Custom Computing Machines (FCCM)*. 1–9. <https://doi.org/10.1109/FCCM53951.2022.9786103>
- [47] Wesley W Terpstra. 2017. TileLink: A free and open-source, high-performance scalable cache-coherent fabric designed for RISC-V. In *Proc. 7th RISC-V Workshop*.
- [48] Timely Dataflow 2020. <https://github.com/TimelyDataflow/timely-dataflow>
- [49] Tianrui Wei, Nazerke Turtayeva, Marcelo Orenes-Vera, Omkar Lonkar, and Jonathan Balkind. 2023. Cohort: Software-Oriented Acceleration for Heterogeneous SoCs. In *Proceedings of the 28th ACM International Conference on Architectural Support for Programming Languages and Operating Systems, Volume 3* (<conf-loc>, <city>Vancouver</city>, <state>BC</state>, <country>Canada</country>, </conf-loc>) (*ASPLOS 2023*). Association for Computing Machinery, New York, NY, USA, 105–117. <https://doi.org/10.1145/3582016.3582059>
- [50] Ying Wei, Yi Chieh Huang, Haiming Tang, Nithya Sankaran, Ish Chadha, Dai Dai, Olakanmi Oluwole, Vishnu Balan, and Edward Lee. 2023. 9.3 NVLink-C2C: A Coherent Off Package Chip-to-Chip Interconnect with 40Gbps/pin Single-ended Signaling. In *2023 IEEE International Solid-State Circuits Conference (ISSCC)*. 160–162. <https://doi.org/10.1109/ISSCC42615.2023.10067395>
- [51] Xilinx DMA Benchmark 2024. [https://github.com/Xilinx/dma\\_ip\\_drivers/tree/master](https://github.com/Xilinx/dma_ip_drivers/tree/master)
- [52] Hanqing Zeng and Viktor Prasanna. 2020. GraphACT: Accelerating GCN Training on CPU-FPGA Heterogeneous Platforms. In *Proceedings of the 2020 ACM/SIGDA International Symposium on Field-Programmable Gate Arrays*. ACM, Seaside CA USA, 255–265. <https://doi.org/10.1145/3373087.3375312>